Generation of Free Radicals by Emodic Acid and its [d-Lys^6]GnRH-conjugate

Author(s): Shai Rahimipour, Izhak Bilkis, Vincent Péron, Georg Gescheidt, Frédérique Barbosa, Yehuda Mazur, Yitzhak Koch, Lev Weiner, and Mati Fridkin
Source: Photochemistry and Photobiology, 74(2):226-236.
Published By: American Society for Photobiology
DOI: http://dx.doi.org/10.1562/0031-8655(2001)074<0226:GOFRBE>2.0.CO;2
URL: http://www.bioone.org/doi/full/10.1562/0031-8655%282001%29074%3C0226%3AGOFRBE%3E2.0.CO%3B2

Photochemistry and Photobiology, 2001, 74(2): 226–236

Generation of Free Radicals by Emodic Acid and its [D-Lys^6]GnRH-conjugate¶

Shai Rahimipour[1,2], Izhak Bilkis[3], Vincent Péron[4], Georg Gescheidt*[4], Frédérique Barbosa[5], Yehuda Mazur[1], Yitzhak Koch[2], Lev Weiner[1] and Mati Fridkin*[1]

Departments of [1]Organic Chemistry and [2]Neurobiology, The Weizmann Institute of Science, Rehovot, Israel; [3]Institute of Biochemistry, Food Science and Nutrition, Faculty of Agriculture, Hebrew University, Rehovot, Israel; [4]Institut für Physikalische Chemie, Universität Basel, Klingelbergstrasse, Basel, Switzerland and [5]Institut für Organische Chemie, Universität Basel, St. Johanns, Basel, Switzerland

Received 30 January 2001; accepted 7 May 2001

ABSTRACT

In an attempt to develop an efficient chemotherapeutic agent targeted at malignant cells that express receptors to gonadotropin releasing hormone (GnRH) we coupled [D-Lys^6]GnRH covalently to an emodin derivative, i.e. emodic acid (Emo) to yield [D-Lys^6(Emo)]GnRH. Emodin is a naturally occurring anthraquinone which is widely used as a laxative and has other versatile biological activities. Physico-chemical studies employing electron paramagnetic resonance and electrochemistry of the conjugate as well as the (Emo) moiety showed that these compounds could be easily reduced either chemically, photochemically or enzymatically to their corresponding semiquinones. In the presence of oxygen the semiquinones generated reactive oxygen species (ROS), mainly superoxide and hydroxyl radicals, which were detected by the spin trapping method. Moreover, upon irradiation with visible light these compounds produced ROS and a highly reactive excited triplet state of Emo, which by itself may cause the oxidation of certain electron acceptors such as amino acids and bases of nucleic acids. Thus, [D-Lys^6]GnRH-photosensitizer conjugates may be potentially used for targeted photodynamic chemotherapy aimed at treating cancer cells that carry GnRH receptors. These conjugates may also induce cytotoxicity in the dark similar to common conventional chemotherapeutic agents. The peptidic moiety, [D-Lys^6]GnRH, was found to be stable toward highly reactive ROS generated either from enzymatic reduction or upon photoirradiation. The physico-chemical properties of Emo were only marginally influenced by the peptidic [D-Lys^6]GnRH carrier.

INTRODUCTION

Hydroxylated 9,10-anthraquinones are abundant compounds that are used in diverse fields. They display marked pharmacological activities, and are most notably used as anticancer and antimicrobial drugs (1). Hydroxylated anthraquinones are characterized by two features: (a) they possess remarkable stability toward light, which is attributed to the rapid deactivation of the excited state into the ground state (2); and (b) they are efficient electron acceptors. The presence of the hydroxyl groups in the 1,4 or 1,8 positions leads to strong intramolecular hydrogen bonding (Fig. 1). Consequently, the negative charge at the site of the carbonyl oxygen atoms in the semiquinone state is counterbalanced, thus shifting the reduction potential to less negative values. Accordingly, certain hydroxylated anthraquinones can undergo electron-transfer reactions with flavoenzymes, *e.g.* reduced nicotinamide adenine dinucleotide phosphate (NADPH)†-cytochrome P450 reductase, to yield the corresponding semiquinone (3). Electron transfer from the semiquinone to molecular oxygen leads to the generation of the superoxide radical anion ($O_2^{\cdot-}$) from which hydrogen peroxide (H_2O_2) and the hydroxyl radical ($^{\cdot}OH$) are formed (4). These reactive oxygen species (ROS) oxidize and degrade proteins and nucleic acids within cancer cells (5–7).

Polyhydroxy-9,10-anthraquinones are also known as photosensitizers. Upon irradiation in the presence of molecular oxygen these compounds are able to generate ROS (8). Skin irritation and erythema side effects, which occur in patients treated with certain hydroxylated anthraquinone drugs such

¶Posted on the website on 14 May 2001.

*To whom correspondence should be addressed at (MF): Department of Organic Chemistry, The Weizmann Institute of Science, Rehovot 76100, Israel. Fax: 972-8-9344142; e-mail: mati.fridkin@weizmann.ac.il

*To whom correspondence should be addressed at (GG): Institut für Physikalische Chemie, Universität Basel, Klingelbergstrasse 80, CH-4056 Basel, Switzerland. Fax: 61-2673855; e-mail: georg.gescheidt@unibas.ch

†*Abbreviations:* DMF, dimethylformamide; DMPO, 5,5′-dimethyl-1-pyroline-*N*-oxide; DMSO, dimethyl sulfoxide; $E_{½}$, half reduction potential; Emo, emodic acid; ENDOR, electron-nuclear double resonance; EPR, electron paramagnetic resonance; Fmoc, 9-fluorenylmethoxycarbonyl; GnRH, gonadotropin releasing hormone; hfc, hyperfine coupling constant; HPLC, high-performance liquid chromatography; LH, luteinizing hormone; NADPH, reduced nicotinamide adenine dinucleotide phosphate; NMM, 4-methylmorpholine; NMR, nuclear magnetic resonance; PB, phosphate buffer; PBS, phosphate buffered saline; PyBOP, benzotriazole-1-yl-oxy-tris-pyrrolidino-phosphonium hexafluorophosphate; ROS, reactive oxygen species; SCE, saturated calomel electrode; t_R, HPLC retention time; TFA, trifluoroacetic acid.

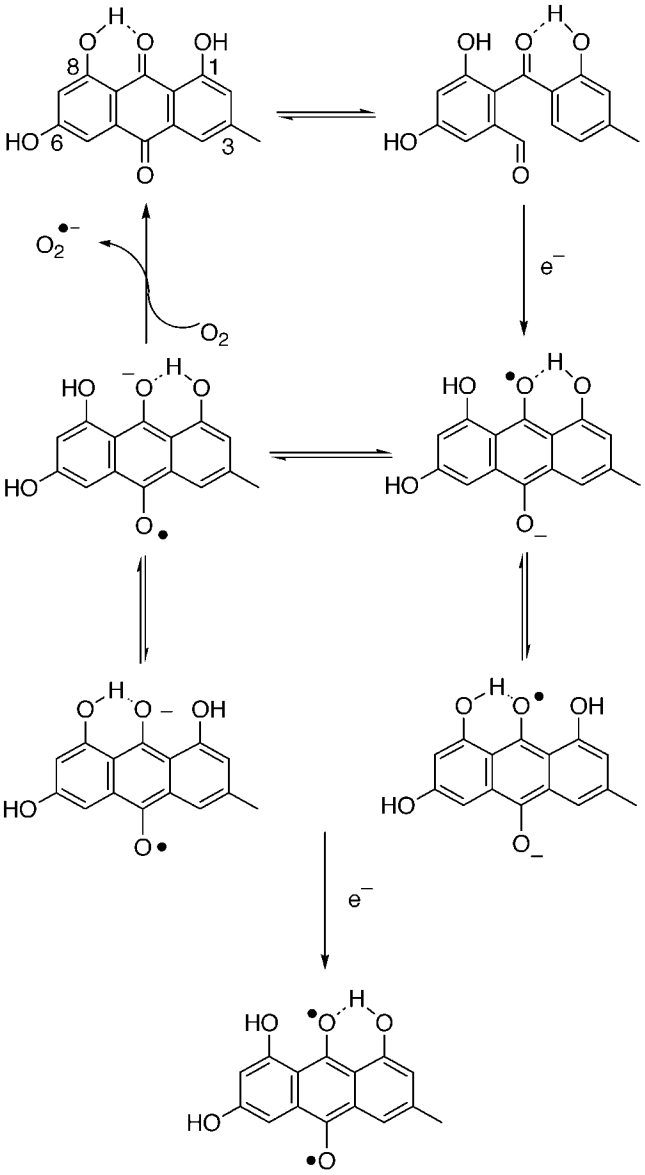

Figure 1. The hydrogen bond structure that contributes to the stabilization of emodin semiquinone generated from one electron reduction. In the presence of molecular oxygen the produced semiquinone could generate the superoxide radical and hydroxyl radical.

as the antipsoriatic agent anthraline, are probably the result of overexposure to sunlight (9).

In the present study we report on the reaction pathways of emodic acid (Emo) **4**, an oxidation product of emodin **1**. Emodin (1,3,8-trihydroxy-6-methyl-9,10-anthraquinone) is a naturally occurring polyhydroxylated anthraquinone widely used in preparing laxatives. It is produced as a secondary metabolite by molds, lichens and other plants and is further metabolized in these species to generate hypericin, a well-known photosensitizer with broad anticancer and antiviral activity (10,11). In addition to mediating the generation of singlet oxygen (type-I photooxidation) (8) emodin can also generate $O_2^{\cdot-}$ upon irradiation (type-II photooxidation) (12).

Several studies have shown that emodin is cytotoxic and mutagenic to some mammalian cell cultures (13–16). Its mode of action is assumed to be partly due to the noncovalent binding of emodin to DNA, the inhibition of topoisomerase II and the inhibiting activity of protein kinase C (17,18). Another conceivable mechanism proposes that the cytotoxicity of emodin could be related to its active metabolite, 2-hydroxy-emodin, which is generated upon the enzymatic hydroxylation of emodin. This hypothesis is based on the observation that 2-hydroxy-emodin is more effective than emodin in generating free radicals and hydrogen peroxide, which eventually cause DNA strand scissions (19). However, these studies showed no evidence for the existence of superoxide, a prerequisite for the generation of hydrogen peroxide.

Treatment of malignancies may often exploit receptors that are preferentially expressed by tumor cells (20). In view of the large and diverse number of tumors that express gonadotropin releasing hormone (GnRH) receptors, targeted chemotherapy has recently gained considerable attention in an attempt to minimize undesired toxicity and afford high drug concentrations at selected, specific loci. GnRH is a key integrator between the neural and the endocrine systems and plays a pivotal role in the regulation of the reproductive system. It is synthesized in hypothalamic neurosecretory cells and provokes the secretion of the gonadotropic hormone from the anterior pituitary. Several studies have demonstrated the existence of high affinity binding sites for GnRH in human prostate cancer as well as in human breast cancer (21,22). Therefore, different analogs of GnRH, agonists as well as antagonists, have been conjugated to cytotoxic compounds such as alkylated nitrogen mustard and anticancer antibiotics such as doxorubicin (23,24). The conjugates exhibited a wide range of specific binding affinities toward GnRH receptors. The cytotoxicity of some peptide–drug hybrids was markedly augmented, *in vitro*, far beyond that of the drug component itself (25–27).

The aims of the present study are the following: (a) to understand the electron-transfer behavior of Emo and its GnRH conjugate using cyclic voltammetry and electron paramagnetic resonance methods such as EPR/electron-nuclear double resonance (ENDOR)/(TRIPLE) electron-nuclear-nuclear triple-resonance; (b) to examine the ability of Emo and its GnRH conjugate to be reduced by NADPH-cytochrome P450 reductase to the corresponding semiquinones, followed by the generation of reactive ROS; (c) to study the photoproducts of Emo and its conjugate by EPR methods; and finally (d) to evaluate the influence of the peptidic carrier, [D-Lys^6]GnRH, on the above properties. The results may have significant potential for the development of Emo-based antineoplastic and antimicrobial drugs.

MATERIALS AND METHODS

All chemicals and reagents were of analytical grade. Rink amide resin, 9-fluorenylmethoxycarbonyl (Fmoc) protected amino acid derivatives and all the reagents for solid-phase peptide synthesis were obtained from Novabiochem (Läufelfingen, Switzerland). Side-chain protecting groups employed were as follows: Arg, 2,2,4,6,7-pentamethyl-dihydrobenzofuran-5-sulfonyl (Pbf); His, trityl (Trt); D-Lys, 4-methyltrityl (Mtt); Trp, *tert*-butyloxycarbonyl (Boc); Ser and Tyr, *tert*-butyl (tBu). 6-Methyl-1,3,8-trihydroxyanthraquinone (emodin) was obtained from Extrasynthese (La Rechassiere Genay, France). 5,5′-Dimethyl-1-pyroline *N*-oxide (DMPO), cytochrome C and NADPH were obtained from Sigma Chemical Co. (St. Louis, MO). Purified NADPH-cytochrome P450 reductase was obtained from Oxford Biomedical Research Inc. (Ann Arbor, MI). The colored

impurity present in the commercial DMPO was removed by treatment with neutral decolorizing charcoal (28). Reversed-phase high-performance liquid chromatography (HPLC) was performed on a Spectra-Physics SP-8800 liquid chromatography system equipped with an Applied Biosystems 757 variable wavelength absorbance detector. HPLC prepacked columns used were: Lichrocart, containing Lichrosorb RP-18 (250 × 10 mm; 7 μm) for semipreparative purification and Lichrospher 100 RP-18 for analytical purposes (250 × 4 mm; 5 μm), Merck (Darmstadt, Germany). HPLC purification and analyses were achieved by using 0.1% trifluoroacetic acid (TFA) in water as buffer A and 0.1% TFA in 75% aqueous acetonitrile as buffer B. Eluent composition was 10% B for the first 10 min and increased linearly to 100% B 50 min after the injection time. Nuclear magnetic resonance (NMR) spectra were recorded at 5°C on Brucker spectrometers (270 and 500 MHz). Mass spectrometry was performed on a Micromass Platform LCZ 4000 (Manchester, UK) utilizing electron spray ionization method. For amino acid composition analysis peptides were hydrolyzed in 6 *N* HCl at 100°C for 24 h under vacuum, and the hydrolyzates were analyzed with a Dionex Automatic Amino Acid Analyzer.

1,6,8-Trihydroxy-3-carboxylic acid-anthraquinone (emodic acid)

Emodin **1** (4 g, 14.8 mmol) was acetylated by acetic anhydride (40 mL) and a catalytic amount of H_2SO_4 (0.8 mL) at 60°C for 40 min. The resulting yellow precipitate (5 g, 85% yield) was filtered, washed with H_2O and dried. A solution of crude triacetylemodin **2** (3 g, 7.57 mmol) in acetic acid (125 mL) and acetic anhydride (125 mL) was then oxidized with a solution of CrO_3 (2 g, 20 mmol) and dissolved in water (5 mL) and acetic acid (60 mL) at 70°C for 3.5 h. Next, the green solution thus obtained was concentrated (to 250 mL), hot water (1200 mL) was then added, and the solution was refrigerated overnight. The residue was filtered, washed with cold water and dried to yield triacetylemodic acid **3** with an 84% yield. Finally, the acetyl groups were hydrolyzed with 2 *M* NaOH (100 mL) at 80°C for 2 h. After acidification and filtration Emo **4** was obtained with an 85% yield and used directly for conjugation with [D-Lys^6]GnRH. HPLC retention time (t_R): 43 min. ^{1}H NMR (270 MHz; methanol-d_4): δ = 6.62 (d, 1H), 7.26 (d, 1H), 7.84 (d, 1H), 8.3 (d, 1H). Mass spectrometry: found *m/z* $[M - H]^+$ = 298.7; calcd for $C_{15}H_8O_7$ $[M - H]^+$ = 299. UV–vis (dimethyl sulfoxide [DMSO]): λmax/nm (log ϵ), 290 (4.19), 445 (3.98).

[D-Lys^6(6-oxy-1,3,8-trihydroxy anthraquinone)]GnRH ([D-Lys^6(Emo)]GnRH)

[D-Lys^6]GnRH was synthesized on an automatic multiple peptide synthesizer (AMS-422, Abimed Analysen-Technik GmbH, Langenfeld, Germany) with Rink amide resin as a polymeric support following the company's protocol for Fmoc strategy as described (29,30). To a dimethylformamide (DMF) solution (1 mL) of the dried peptide (31 mg, 25 μmol) and Emo (8.25 mg, 27.5 μmol) containing 4-methylmorpholine (NMM) (8.2 μL, 75 μmol), a DMF solution (0.5 mL) of benzotriazole-1-yl-oxy-tris-pyrrolidino-phosphonium hexafluorophosphate (PyBOP) (13 mg, 27.5 μmol) was added. The mixture was stirred for 2 h at room temperature. The progress of the reaction was followed by the disappearance of [D-Lys^6]GnRH as revealed by analytical HPLC. Upon completion of the reaction the crude peptide was precipitated with ice-cold *tert*-butyl methyl ether (10 mL), collected by centrifugation and dried. It was then purified to homogeneity by semipreparative HPLC to yield 23 mg (15 μmol; 60%). HPLC (t_R): 39.1 min (t_R = 31.6 min for [D-Lys^6]GnRH in the same conditions). ^{1}H NMR (500 MHz; H_2O:D_2O, 9:1; pH 3.1, the partial assignment was based on 2D Nuclear overhauser effect, nuclear overhauser enhancement spectroscopy and Homonuclear Hartman Hann Spectroscopy): δ = 0.85 (d, 3H, Leu), 0.90 (d, 3H, Leu), 1.54–1.57 (m, 6H, Leu, Arg, Pro, pGlu), 1.64 (m, 4H, Leu, Arg, Pro, Lys), 1.74 (m, 2H, Arg, Lys), 1.82 (m, 1H, Lys), 2.43 (m, 1H, Tyr), 2.59 (m, 1H, Tyr), 2.81 (d, 1H, Tyr), 2.9 (m, 3H, Trp, His), 3.42 (m, 1H, Pro), 3.53 (m, 2H, Ser, Pro), 3.59 (m, 1H, Ser), 3.82 (d, 1H, Gly), 3.85 (d, 1H, Gly), 4.15 (m, 1H, pGlu), 4.23 (m, 2H, Ser, Tyr), 4.34 (m, 3H, Leu, Pro, Lys), 4.48 (m, 2H, Arg, Trp), 4.55 (br, 1H, His), 6.31 (s, 1H, Tyr), 6.38 (d, 1H, Emo), 6.49 (br, 1H), 6.62 (s, 1H, Tyr), 6.69 (d, 1H, Emo), 6.77 (s, 1H, Trp), 6.91 (d, 1H, Emo), 7.0 (d, 1H, Emo), 7.10 (s, 1H, His), 7.17 (d, 2H, Arg), 7.18 (s, 1H, Trp), 7.35 (s, 1H, Trp), 7.51 (s, 1H, Trp), 7.56 (s, 1H, Trp), 7.91 (br, 1H, Tyr), 7.96 (d, 1H, Trp), 8.20 (d, 1H, Ser), 8.34 (s, 1H, His), 8.39 (d, 1H, Leu), 8.49 (d, 1H, Arg), 8.53 (d, 1H, His), 8.64 (s, 1H, Gly), 8.36 (d, 1H, Lys). Mass spectrometry: found *m/z* $[M + H]^+$ = 1536.17; calcd for $C_{74}H_{91}N_{18}O_{19}$ $[M + H]^+$ = 1536.62. Amino acid analysis after hydrolysis with 6 *M* HCl at 110°C for 22 h: Glu 1.00, His 1.00, Ser 0.87, Tyr 0.98, Lys 1, Leu 0.98, Arg 1.05, Pro 1.01, Gly 0.98. Trp could not be detected due to its destruction under the acidic conditions of hydrolysis. UV–vis (DMSO): λ_{max}/nm (log ϵ), 285 (4.28), 443 (4).

Electrochemistry

Cyclic voltammetry was measured on a Metrohm Polarecord E 506 and a VA scanner E 612 with a VA stand 663 (Metrohm AG, Herisau, Switzerland). All measurements were carried out in DMF (kept over molecular sieves) as a solvent containing 0.1 *M* tetra-*n*-butylammonium perchlorate (*n*-Bu_4NClO_4, Fluka, Buchs, Switzerland, dried overnight at 100°C before using) as a supporting electrolyte at room temperature. The working electrode was a hanging mercury drop, whereas glassy carbon was used as a counter electrode and an Ag wire served as the reference electrode. All the reported potentials were cited against a saturated calomel electrode (SCE). Benzophenone was used as an internal standard ($E_{½}$ = −1.80 V *vs* SCE) where $E_{½}$ is the half reduction potential (31).

EPR and ENDOR studies of radicals generated by the reduction of Emo and its [D-Lys^6]GnRH conjugate

Chemical and electrochemical reduction. For EPR and ENDOR spectroscopy Emo and its GnRH conjugate were reduced to the corresponding semiquinone with Zn in DMF or with Zn in DMSO-d_6/D_2O (10:1; vol/vol). Reduction was also carried out electrochemically at 0°C on a helical gold cathode using platinum wire as the counter electrode. Reductions were performed either in DMF containing 0.1 *M* tetra-*n*-butylammonium perchlorate as a supporting electrolyte or in phosphate buffered saline (PBS, pH 7.4). Electron spin resonance measurements were performed by a Varian-E9 instrument, and a Bruker-ESP-300 (Bruker, Karlsruhe, Germany) system was used for all ENDOR and TRIPLE-resonance studies. Simultaneous recording of the electronic absorption bands was performed on a J&M TIDAS-16 instrument (J&M, Aalen, Germany), which was attached directly to the optical cavity of the EPR spectrometer (32).

Enzymatic reduction. The activity of the reductase was determined spectrophotometrically from the kinetic measurements of reduced cytochrome C production at 550 nm (33). The formation of superoxide or hydroxyl radicals by enzymatic reduction was followed by the spin trapping technique. The reaction mixture (final concentration) consisted of NADPH-cytochrome P450 reductase (0.1–0.2 unit/mL), NADPH (1 m*M*), $FeCl_3$ (0.1 m*M*), ethylenediamine-tetraacetic acid (0.2 m*M*), DMPO (50–100 m*M*), Emo or its corresponding [D-Lys^6]GnRH analog (0.1 m*M*) in PBS, in the presence or absence of 10% DMSO. Measurements were made in a 200 μL EPR flat cell at 22°C.

Photoreduction of Emo and [D-Lys^6(Emo)]GnRH. All irradiations were carried out with a KL 1500 electronic projector lamp (Schott, Mainz, Germany). Unless otherwise stated, all irradiations were carried out with an appropriate filter with a bandpass of 320–510 nm and λ_{max} = 400 nm. Samples were irradiated directly inside the EPR cavity with an optical fiber while the EPR spectra was recorded. Emo semiquinone was generated under anaerobic conditions by the irradiation of Emo (2 m*M*) in DMF containing 5% triethylamine (vol/vol). For spin trapping studies a mixture of DMPO (0.1 *M*), Emo (1, 0.1 m*M*) or the corresponding [D-Lys^6]GnRH analog (0.1 m*M*) in the specified solvent and pH was irradiated in a 200 μL EPR flat cell. To generate anaerobic conditions Argon was bubbled through the corresponding sample 10 min before measurements. All spin trapping studies were performed with a Bruker Electron Spin Resonance ER200D-SRC spectrometer at 25°C.

Simulation of EPR spectra. For computer simulations of the EPR spectra the public domain program WINSIM (NIEHS, NIH, Research Triangle Park, NC) was used (34).

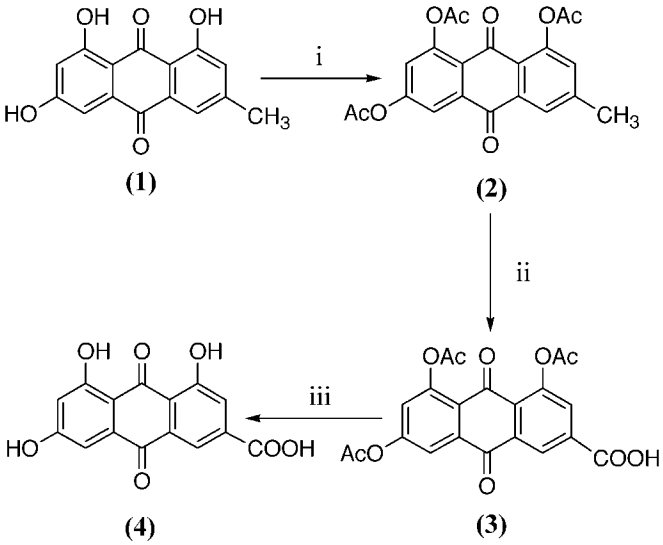

Figure 2. Synthetic pathway to Emo. (i) Acetic anhydride, H_2SO_4 (catalytic), 60°C, 40 min; (ii) CrO_3, acetic anhydride:acetic acid (1:1), 60°C, 3.5 h; (iii) $NaOH/H_2O$, reflux, 2 h.

Quantum mechanical calculations. Quantum mechanical calculations of Emo were performed with the GAUSSIAN94 package (Gaussian Inc., Pittsburgh, PA). The geometry was optimized by the UHF-3-21G* method, whereas the isotropic hyperfine coupling constants (hfc's) were determined by a single-point calculation of the density functional level of theory (UB3LYP/6-31G*) (35–37).

RESULTS AND DISCUSSION

Synthesis

Emo **4** was synthesized (Fig. 2) from commercially available emodin **1**, as described in the 'Materials and Methods' section and used without any further purification for conjugation to [D-Lys^6]GnRH.

The synthesis of [D-Lys^6(Emo)]GnRH involves the reaction of [D-Lys^6]GnRH in a homogeneous solution with Emo employing PyBOP as a coupling reagent in presence of NMM as a base (Fig. 3). The conjugate was purified to homogeneity (≥97%) by semipreparative HPLC and characterized by analytical HPLC, UV, mass spectrometry and amino acid analysis. This method is a 'one-pot synthesis' which results in better yield (>60%) and purity as compared with other methods that use active esters such as *N*-hydroxysuccininide as coupling reagents (30). The efficacy of this method may be attributed to the minimization of side reactions such as those occurring at the hydroxylic function of Tyr and Ser.

Biological evaluation

To determine the ability of [D-Lys^6(Emo)]GnRH to bind selectively to GnRH receptor we performed competitive binding assays (38). The results demonstrate that [D-Lys^6(Emo)]GnRH binds to GnRH receptors with relatively high affinity (2.5×10^{-10} *M*) although it is reduced by about three times compared to the parent peptide (0.8×10^{-10} *M*). Moreover, upon its binding to the anterior pituitary cells [D-Lys^6(Emo)]GnRH induced the release of luteinizing hormone (LH) from these cells at the same range of concentration as [D-Lys^6]GnRH (39).

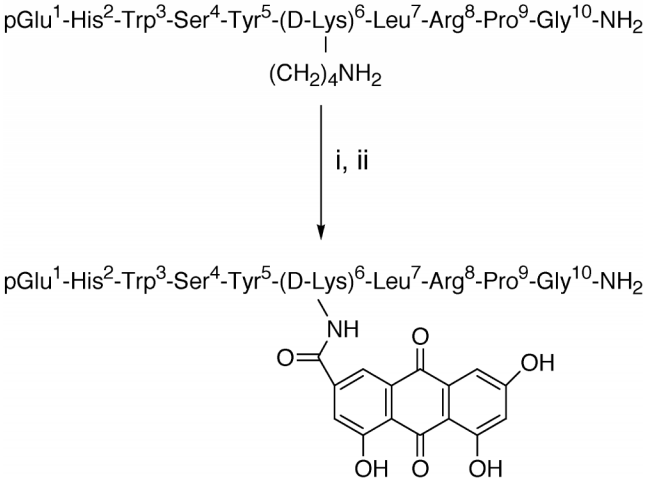

Figure 3. Synthesis of [D-Lys^6(Emo)]GnRH in homogeneous solution. (i) Emo, PyBOP and NMM in DMF at room temperature for 2 h. (ii) HPLC purification (RP-18).

Electrochemistry

The mode of action of antitumor quinones presumably involves their participation in redox cycling (1). After their enzymatic reduction to the corresponding semiquinones these quinones can mediate the production of superoxide. Obviously, these reactions are possible only for those quinones possessing redox potentials that can be achieved in biological systems. Therefore, to evaluate this parameter we determined the redox potential of Emo (Fig. 4). The voltammogramm shows two quasi-reversible redox steps whose shape does not depend on the scan rate (50–400 mV/s). Table 1 lists the half-wave potentials, $E_{½}$, of Emo. For a comparison the cyclic voltammogramm of emodin was also recorded. For both the compounds the first reduction wave occurs at $E^1_{½} = -0.59$ V (*vs* SCE) resembling the values of related polyhydroxylated anthraquinones (3) such as adriamycin with $E^1_{½} = -0.665$ V (*vs* SCE). A second reduction step of Emo occurs at $E^2_{½} = -1.31$ V (*vs* SCE), a value which is 200 mV more negative than that of emodin. This difference can be attributed to the presence of the dissociated COOH group in the Emo. The two waves at $E^1_{½}$ and $E^2_{½}$ represent the reduction of Emo (emodin) to the corresponding semiquinone and dianion, respectively (Fig. 1).

EPR/ENDOR measurements

The structure of the Emo semiquinone (radical anion) was established by means of EPR/ENDOR experiments. The semiquinone radical anions were generated either by chemical, electrochemical or photochemical reduction. Contact of a DMF solution containing Emo with a Zn mirror or its electrochemical reduction at an Au anode (see 'Materials and Methods') led to well-resolved EPR spectra (Fig. 5). The spectra were detectable even after a period of several weeks at room temperature. This observation suggests considerable persistence of the radical anion of Emo. From the same sample subjected to Zn reduction a well-defined ENDOR spectrum was apparent. The isotropic hfc thus obtained (Fig. 5) allowed the simulation of the EPR spectra.

In addition, Emo was Zn-reduced in DMSO-d_6 containing

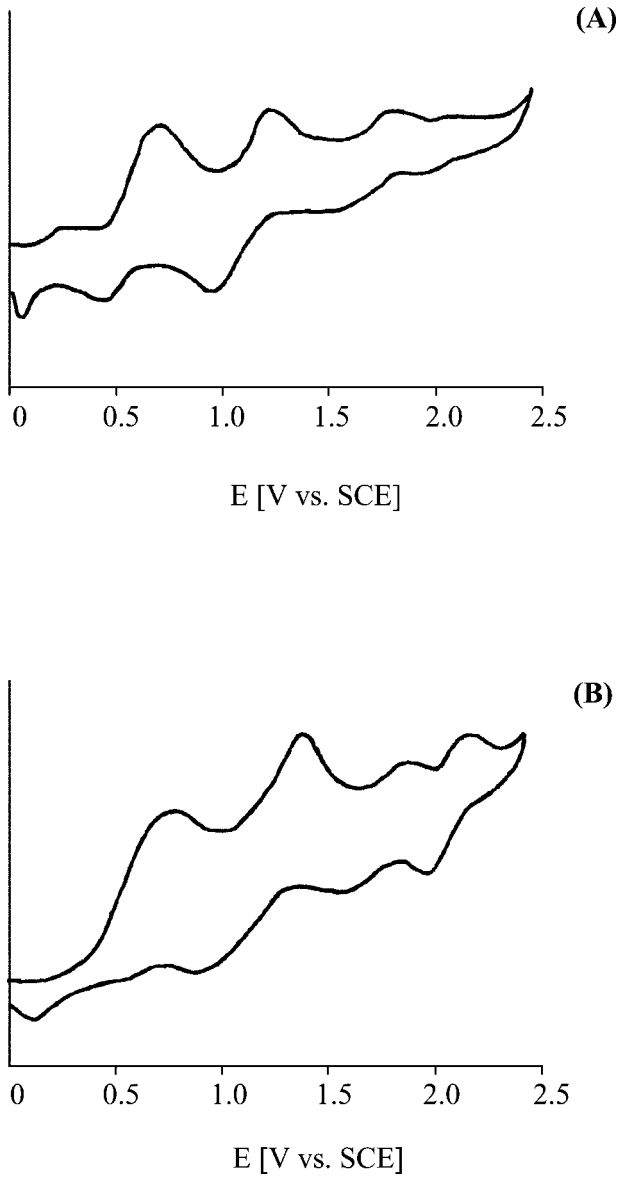

Figure 4. Cyclic voltammograms of: (a) emodin and (b) Emo in DMF containing 0.1 *M* tetra-*n*-butylammonium perchlorate. Benzophenone was used as an internal standard ($E_{½}$ = −1.8 V *vs* SCE).

10% D_2O (Fig. 5). These conditions led to a H/D exchange at the hydroxyl groups and assisted the assignments of hfc. The ENDOR spectra obtained using the DMF and D_2O/DMSO-d_6 mixtures as a solvent were virtually identical. This finding suggests that the three symmetrically nonequivalent hydroxy protons possess hfc which are surprisingly identical to the hfc of protons that are not exchangeable (α-protons). However, a comparison of the EPR spectra using DMF and D_2O/DMSO-d_6 reveals systematic differences. More specifically, the overall width of the spectra and the distance between the three line groups are nearly identical. The primary deviation, however, is the different number of small splittings in the line groups. Accordingly, only the lowest proton hfc (0.168 G) is missing for the DMSO-d_6 solution. Therefore, the hfc of the hydroxy protons are identical to the lowest α-proton hfc. Table 2 summarizes the hyperfine data.

Table 1. Reduction potentials of emodin and emodic acid in DMF in V *vs* SCE

Redox potential	Emodic acid	Emodin
$E^{(1)}_{1/2}$	−0.59	−0.59
$E^{(2)}_{1/2}$	−1.31	−1.11

EPR study of the [D-Lys^6(Emo)]GnRH analog

Direct detection of peptide–semiquinone radicals produced by chemical or electrochemical reduction is generally difficult. This is presumably because of the high sensitivity of the amino acid residues to reactive metals (such as potassium or zinc), fast quenching reactions of the semiquinone radical anion by amino acid residues or the low solubility of the peptide–quinone conjugates in most organic solvents (such as tetrahydrofuran). The [D-Lys^6]GnRH analogs were found to be highly stable toward ROS (30) and have a pronounced

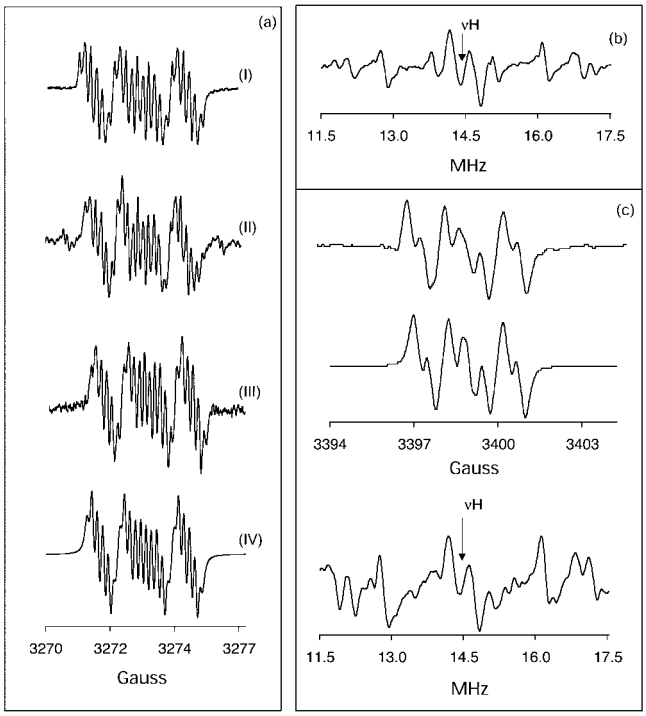

Figure 5. (a) EPR spectra of Emo semiquinone generated from I: reduction of Emo with zinc in DMF. EPR conditions: microwave power, 3.0 mW; modulation amplitude, 0.032 G; receiver gain, 1.25 × 10^4; time constant, 1.0 s; scan range, 20 G; temperature, 25°C. II: photolysis in DMF/triethyl amine (95:5). EPR conditions: microwave power, 10 mW; modulation amplitude, 0.11 G; receiver gain, 1 × 10^6; time constant, 0.32 ms; scan range, 10 G; temperature, 25°C. III: electrolysis in DMF. EPR conditions: microwave power, 5 mW; modulation amplitude, 0.05 G; receiver gain, 1.25 × 10^4; time constant, 1.0 s; scan range, 10 G; temperature, 25°C. IV: simulation of the EPR spectrum; coupling constants are given in Table 2. (b) Corresponding proton–ENDOR spectrum at −30°C. (c) Top: reduction with zinc in DMSO-d_6/D_2O (10:1). EPR conditions: microwave power, 2 mW; modulation amplitude, 6.3 mG; receiver gain, 1.25 × 10^4; time constant, 1.0 s; scan range, 10 G; temperature, 25°C. Center: computer simulation. Bottom: corresponding proton-ENDOR spectrum.

Table 2. EPR data of emodic acid and [D-Lys^6(Emo)]GnRH and calculated hfc's (UB3LYP/6-31G*//UHF/3-21G*); hfc's in G; for numbering see structure in Fig. 1

	Emodic acid			[D-Lys^6 (Emo)] GnRH	Emodic acid
Position	Zn/DMF	Irradiation	Zn/DMSO-d_6/D_2O	Zn/DMF	Calc
OH (1)	0.168	0.16	—	0.168	+0.46
H (2)	1.868	1.83	1.868	1.855	−2.23
COOH (3)	—	—	—	—	+0.24
H (4)	1.141	1.1	1.141	1.234	−0.88
H (5)	0.374	0.37	0.374	0.374	−0.57
OH (6)	—	—	—	—	+0.25
H (7)	0.179	0.17	0.179	0.179	+0.31
OH (8)	0.168	0.16	0.168	0.168	−0.32
g factor	2.00415	2.00415	2.00415	2.00410	—

solubility in DMF solutions. Thus, together with the high thermodynamic and kinetic stability of the semiquinone of Emo in DMF, it is likely that [D-Lys^6(Emo)]GnRH may be reduced chemically by employing Zn in DMF. Indeed, such a reduction of [D-Lys^6(Emo)]GnRH gave rise to a partly resolved EPR spectrum (Fig. 6), which could be attributed to the slow rotation of the molecule. The EPR spectrum persisted for several days even at room temperature. The same EPR spectrum was also obtained upon electrolysis in DMF. The EPR simulation was achieved with the same hfc established for the Emo semiquinone but with a broader linewidth (Table 2).

The rather similar values of the proton-coupling constants and *g*-factors obtained for [D-Lys^6(Emo)]GnRH semiquinone and the free Emo suggest that the parent peptide has only a marginal influence on the electron-transfer pathways of Emo. This may be due to the β-turn structure of [D-Lys^6]GnRH in which the amino acid residue in position 6 is exposed (40,41). Thus, the Emo at the side chain of D-Lys^6 is remote from the peptide moiety and, therefore, the two distinct molecular entities do not affect each other. Indeed, [D-Lys^6(Emo)]GnRH was found to compete with the parent peptide for the same GnRH receptor binding site and to induce LH secretion from primary rat pituitary cell culture at the same range of concentrations (39).

Structure of the Emo semiquinone radical anion

The experiments described indicate that the Emo semiquinone radical anion has considerable stability, and helps to assign the hydroxy-proton hfc. However, questions remain concerning the assignment of the remaining hfc, the reason for the marginal differences between the data obtained for parent and the [D-Lys^6(Emo)]GnRH semiquinone and the electronic structural features that lead to the persistence of the radical anions. These questions may be answered, at least in part, by quantum mechanical calculations. Various independent publications have recently shown that calculations on the density functional level of the theory provide a valuable insight into the structure of the radicals and radical ions similar to Emo (42,43). Table 2 compares the experimental and the calculated hfc values. Clearly, their agreement is satisfactory. The biggest hfc of 1.868 G is thus assigned to the proton at C(2) and that of 1.14 to H–C(3). The remaining

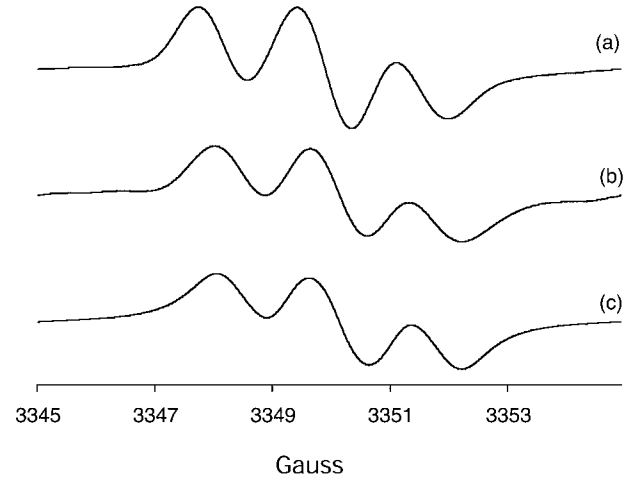

Figure 6. EPR spectrum of [D-Lys^6(Emo)]GnRH semiquinone generated from: (a) reduction of [D-Lys^6(Emo)]GnRH by Zn/DMF; (b) electrolysis in DMF; (c) computer simulation using the same parameter for Emo (Fig. 5) but with a larger linewidth. EPR conditions: microwave power, 10 mW; modulation amplitude, 0.82 G; receiver gain, 8×10^3; time constant, 0.3 s; scan range, 20 G; temperature, −10°C.

smaller hfc are assigned in descending order according to the predicted values (Table 2). The singly occupied orbital of the semiquinone radical anion is clearly of π type, as shown in Fig. 7. Only a minute amount of spin resides at the carboxyl group at C(3) and the orbital coefficient at this position is exceedingly small. Therefore, no spin can be transferred to substituents at the carboxy group or *vice versa*, substituents at this group have in essence no effect on the electronic properties of the Emo moiety.

Enzymatic reduction

Since the toxicity of quinones is assumed to be directly related to their potential to produce ROS under physiological conditions we examined the ability of Emo and its GnRH conjugate, [D-Lys^6(Emo)]GnRH, to produce ROS by enzymatic reduction. Emo or [D-Lys^6(Emo)]GnRH were incubated with NADPH-cytochrome P450 reductase, NADPH and DMPO (4). The subsequently recorded EPR suggests that in spite of the similarity between Emo and the polyhydroxylated anthraquinones such as adriamycin, Emo and its GnRH conjugate generate ROS only in a modest amount.

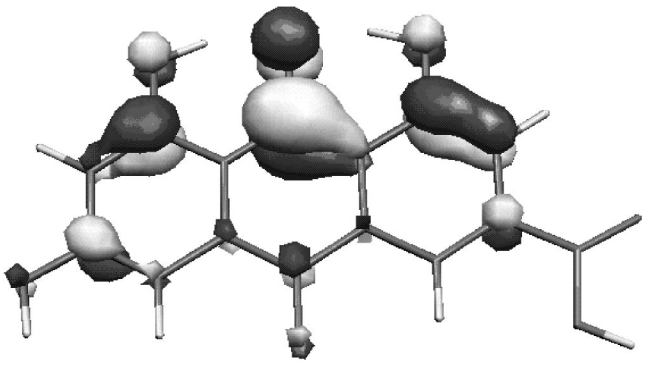

Figure 7. Singly occupied orbital of Emo semiquinone radical anion.

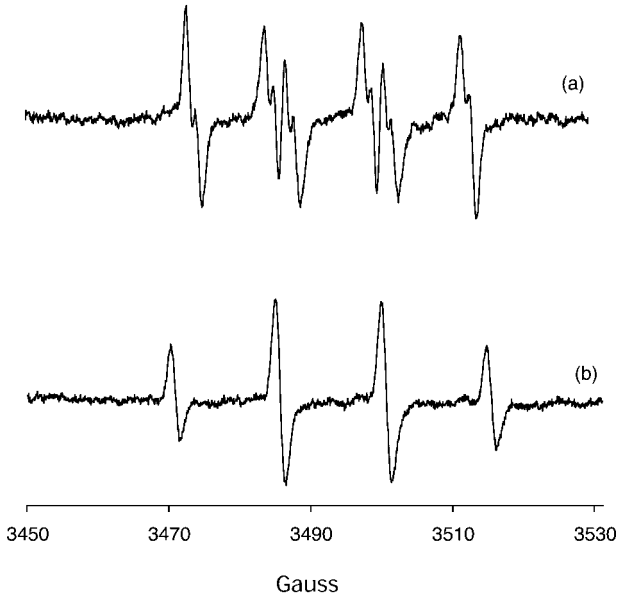

Figure 8. The EPR spectra of the spin adduct DMPO. (a) The spectra of the DMPO–OOH adduct generated by the irradiation of Emo and DMPO in aerated citrate buffer (pH 3) containing 1.4 *M* DMSO. (b) same as (a) but at pH 7.4. The EPR coupling constants are given in Table 3. EPR conditions: microwave power, 20 mW; modulation amplitude, 1.0 and 0.71 G for (a) and (b), respectively; receiver gain, 4×10^5; time constant, 1.25 s; center of field, 3500 G; scan range, 100 G.

Photochemical studies of Emo and [D-Lys^6(Emo)]GnRH

The photoreactivity of Emo and its GnRH conjugate were investigated in aqueous buffer solutions as well as in organic solvents using the spin trapping technique. The influence of iron ions in generating ROS was studied in separate experiments.

Photochemical generation of Emo semiquinone. The generation of semiquinone radicals is a precondition for the formation of ROS (44,45). In this study we succeeded in generating Emo semiquinone by direct irradiation of a DMF solution of Emo in the presence of 5% triethylamine (vol/vol) as an electron donor. This resulted in the appearance of a well-resolved EPR spectrum (Fig. 5). Simulation of the EPR spectrum was achieved with the same hfc's that was established for the Emo semiquinone generated by the reduction with Zn in DMF with minor differences (Table 2). The similarity between the hfc's of semiquinone generated by photoreduction and those obtained by chemical or electrochemical reduction strongly suggests that the structure of the Emo semiquinone thus generated from irradiation is identical to those obtained by other methods.

Photoirradiation of Emo under acidic and basic conditions. When Emo (1 m*M*) and DMPO (0.1 *M*) were irradiated in aerated citrate buffer (20 m*M*, pH 3), a 12-line EPR signal (Fig. 8a) characterized by a DMPO–OOH hyperfine pattern was observed (Table 3). These hfc's are in good agreement with the published data concerning DMPO–OOH adducts (46).

Nevertheless, irradiation of Emo and DMPO in aerated Tris buffer (20 m*M*, pH 7.4) resulted in the generation of a four-line EPR spectrum (Fig. 8b). The characteristic hfc's of the observed signal were similar to those of the DMPO–OH adducts (Table 3).

The spin trapping of $O_2^{\cdot-}$ by DMPO has been reported to occur along with certain artifacts. Specifically, it was shown that the DMPO–OOH adduct could be spontaneously transformed to an adduct that is similar to the DMPO–OH adduct and with the same characteristic hfc (47–49). In order to assure the source of the DMPO–OH adduct (Fig. 8b) the above experiment was repeated in the presence of 10% DMSO. DMSO is known to react with $^{\cdot}OH$ at a high rate to generate $^{\cdot}CH_3$, which can then be trapped by DMPO and identified by its characteristic hyperfine pattern (4). Using a solution containing 1.4 *M* DMSO (10% vol/vol) and 0.1 *M* DMPO and taking into account the bimolecular constants for the interaction of the $^{\cdot}OH$ radical with DMPO (3.4×10^9 M^{-1} s^{-1}) (47) and with DMSO (7×10^9 M^{-1} s^{-1}) (50), only the DMPO–CH_3 spin adduct should be experimentally observed.

$$DMSO + {}^{\cdot}OH \rightarrow {}^{\cdot}CH_3 + HOS(O)CH_3 \quad (1)$$

$${}^{\cdot}CH_3 + DMPO \rightarrow DMPO\text{–}CH_3 \quad (2)$$

However, the addition of 10% DMSO to the tested mixture did not lead to the formation of a DMPO–CH_3 adduct indicating that the production of the DMPO–OH EPR spectrum (Fig. 8b) was not because of the trapping of the $^{\cdot}OH$ radical. Moreover, adding superoxide dismutase decreased the observed signal by up to 50% (Fig. 9), and addition of catalase did not appreciably affect the EPR intensity (data

Table 3. The EPR parameters of the DMPO spin adduct generated from the irradiation of emodic acid under different conditions.

Solvent*	pH	Irradiation wavelength†	Radical tapped	Hyperfine splitting constant (G)		
				a_N	a_H^{β}	a_H^{γ}
Tris buffer	7.4	320–510 nm	$^{\cdot}OH$	14.9	14.9	
Citrate buffer	3	320–510 nm	$O_2^{\cdot-}$	14.08	11.18	1.21
Citrate buffer + 0.1 m*M* Fe(II)	3	Dark	CH_3	16.6	22.6	
Ethanol		320–510 nm	$^{\cdot}OC_2H_5$	13.7	7.54	1.62
			$O_2^{\cdot-}$	13.29	10.2	1.42
Ethanol		All	$^{\cdot}OC_2H_5$	13.7	7.54	1.6
			$O_2^{\cdot-}$	13.42	10.1	1.44
			—	13.7		

*Aqueous solvents contained 10% DMSO.
†All: unfiltered light from a tungsten lamp.

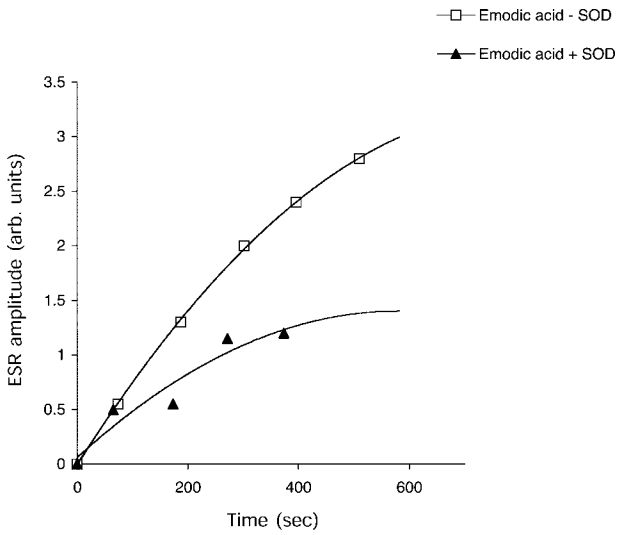

Figure 9. The effect of SOD on the spin adduct generated from the irradiation of Emo (1 m*M*) and DMPO (0.18 *M*) in aerated PBS in the presence or absence of 0.15 mg of SOD. The accumulative kinetics of the spin adduct was measured from the intensity of the second component of the quartet.

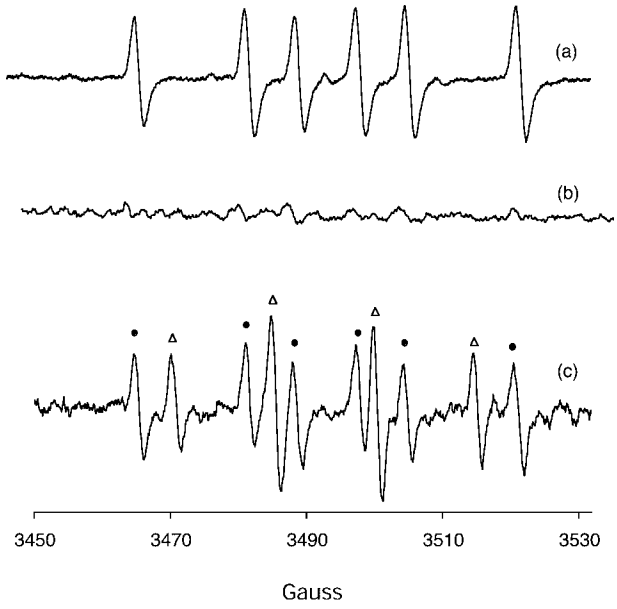

Figure 10. EPR spectra of Emo and DMPO in aerated citrate buffer. (a) EPR spectrum at dark condition immediately after addition of Fe(II). (b) same as (a) after treatment with Fe(II) in the dark for 20 min. Spectrum (c) was obtained after irradiation of (b). DMPO–CH_3 is indicated as (●) and DMPO–OH as (△). EPR conditions: microwave power, 20 mW; modulation amplitude, 1.0 G; receiver gain, 5×10^5; time constant, 1.25 s; scan range, 100 G; center of field, 3500 G; temperature, 25°C.

not shown). These results suggest that the observed DMPO–OH adduct presumably stems from the decomposition of DMPO–OOH (48,51,52). This explanation could be based on the nucleophilic addition of the HO^- to DMPO under basic conditions (pH 7.4) followed by electron-transfer processes (53,54).

The rate of DMPO–OOH production in aqueous solution is mainly dependent on (a) the dismutation rate of $O_2^{\cdot-}$ (reaction 3); (b) the reaction rate of $O_2^{\cdot-}$ with DMPO (reaction 4); and (c) the decomposition rate of DMPO–OOH to DMPO–OH (reaction 5).

$$O_2^{\cdot-} + O_2^{\cdot-} + 2H^+ \rightarrow H_2O_2 + O_2 \quad (3)$$

$$O_2^{\cdot-} + \text{DMPO} + H^+ \rightarrow \text{DMPO–OOH} \quad (4)$$

$$\text{DMPO–OOH} \rightarrow \text{DMPO–OH} \quad (5)$$

The dismutation rate of $O_2^{\cdot-}$ (reaction 3) is known to be pH dependent, being increased as the pH decreases (55). However, the reaction rate of the competitive reaction, DMPO with $O_2^{\cdot-}$, is also enhanced at a decreased pH (47). Moreover, the DMPO–OOH adduct is assumed to be more stable at a reduced pH, which is reasonable when it is considered as an organic peroxide. For example, the half-life-time of the DMPO–OOH EPR signal at pH 5 is about three times longer than pH 8 (28). Thus, it is concluded that the high rate of reaction 4 and the low rate of reaction 5 are responsible for the observation of DMPO–OOH under acidic conditions.

Effect of iron ions on the generation ROS. It is well established that iron ions and their complexes, which are present in most biological systems, play an important role in the generation of ROS (56). To evaluate the influence of Fe(II) on the photogeneration of ROS by Emo the above related experiments were repeated in the presence of Fe(II). Adding Fe(II) (0.1 m*M*) to the acidic mixture of Emo, DMPO and 10% DMSO in the dark resulted in a six-line EPR spectrum (Fig. 10a) stemming from the DMPO–CH_3 adduct (Table 3). The DMPO–CH_3 adduct is a product of the reaction of DMSO with $^{\cdot}OH$ (Eqs. 1 and 2), a radical formed by the Fe(II) catalyzed decomposition of a residue trace of H_2O_2 (Fenton-type reaction). The trace of H_2O_2 in the solution could have been accumulated when the stock solution of Emo was exposed to light before its measurement (19). Further evidence for the existence of H_2O_2 in the aqueous solution of Emo is based on the observation that irradiation of the acidic mixture of Emo, DMSO and DMPO under anaerobic conditions with unfiltered light also results in the formation of the DMPO–CH_3 adduct. One possible explanation for detecting a DMPO–CH_3 adduct under anaerobic conditions could be the decomposition of H_2O_2 by ultraviolet light (57).

Although the irradiation of an acidic mixture of Emo and DMPO led only to the generation of a DMPO–OOH adduct (Fig. 8a), without the appearance of any other adducts, the addition of Fe(II) to this mixture resulted in the formation of a different EPR spectrum stemming from two dominating spin adducts, namely, DMPO–OH and DMPO–CH_3 (Fig. 10c). Note that in order to decompose the H_2O_2 traces present in the Emo mixture the Emo solution was pretreated with Fe(II) before adding DMPO and subjecting it to irradiation (Fig. 10b). The observed spin adducts were presumably generated from a Fenton-type decomposition of a DMPO–OOH adduct to a DMPO–OH adduct and $^{\cdot}OH$ (Eq. 6) (58,59). The presence of DMSO in the reaction mixture here causes the generation of DMPO–CH_3 adduct (Eqs. 1 and 2).

$$\text{DMPO–OOH} + \text{Fe(II)} \rightarrow \text{DMPO–OH} + {}^{\cdot}OH \quad (6)$$

On the other hand, irradiation of the mixture of Emo,

DMPO and DMSO under basic conditions (Tris buffer 20 m*M*, pH 8), pretreated with Fe(II) in the dark, produced only a four-line EPR spectrum at variance with the acidic conditions. This could be interpreted in terms of faster decomposition of the DMPO–OOH adduct to the DMPO–OH adduct under basic conditions (Eq. 5) rather than its reaction with Fe(II) (Eq. 6). Therefore, the reaction (Eqs. 1 and 2) could not occur under basic conditions.

These results suggest that the observed DMPO–OH spin adduct could be obtained by several other possible ways that do not involve the spin trap interacting with the OH radical. At least 50% of the amount of this radical originated from the decomposition of DMPO–OOH (Fig. 9), and the addition of catalase did not affect significantly the intensity of the DMPO–OH signal. According to the literature two mechanisms should be considered to explain the appearance of the DMPO–OH adduct. The first one involves the addition of a water molecule (hydroxyl ion) to the DMPO with the subsequent oxidation of the obtained hydroxylamine by the parent quinone in the excited state (60) (Eqs. 7–9).

$$\text{Emo} + \text{light} \rightarrow {}^3(\text{Emo}) \tag{7}$$

$$\text{DMPO} + \text{H}_2\text{O} \rightarrow (\text{DMPO–OH}_2) \tag{8}$$

$$(\text{Emo}) + (\text{DMPO–OH}_2) \rightarrow (\text{Emo})^{\cdot -} + (\text{DMPO–OH}) + \text{H}^+ \tag{9}$$

The possibility of oxidation of hydroxylamine (Eq. 8) by the parent quinone (thermal reaction) could be excluded in our case because in dark experiments the DMPO–OH adduct was not formed in detectable amounts. This observation is in accordance with the criteria formulated by Eberson (61) which states that quinones can act as thermal oxidants in the water–DMPO system if their redox potential is >-0.5 V (*vs* SCE). The redox potential of Emo (-0.65 V [*vs* SCE]) is less than this value.

The second possible mechanism involves the oxidation of the spin trap by the parent quinone in the excited state (Eq. 10) followed by the addition of a water molecule (hydroxyl ion) to the obtained radical cation (53,54,61,62) (Eq. 11).

$${}^3(\text{Emo}) + \text{DMPO} \rightarrow (\text{Emo})^{\cdot -} + \text{DMPO}^{\cdot +} \tag{10}$$

$$\text{DMPO}^{\cdot +} + \text{H}_2\text{O} \rightarrow \text{DMPO–OH} + \text{H}^+ \tag{11}$$

In order to examine the possible involvement of at least one of these two mechanisms we carried out our photochemical experiments using two other solvents. Acetonitrile was chosen because of its low nucleophility, ethanol was chosen as the more nucleophilic solvent. Irradiation of Emo and DMPO in aerated ethanol resulted in the appearance of an EPR spectrum, which according to the EPR simulation involves superposition of two radical species, the DMPO–OOH adduct and the DMPO–OCH_2CH_3 adduct (Fig. 11). Such DMPO adducts were observed also following the irradiation of ethanolic solution of 1,8-dihydroxyanthraquinone (9). On the other hand, the irradiation of Emo and DMPO in aerated acetonitrile resulted in the appearance of an EPR spectrum corresponding to the formation of only one radical—the spin adduct of the superoxide radical anion. When 10% of ethanol (vol/vol) was added to the acetonitrile solution of DMPO and Emo the same radical species as in pure ethanol were obtained upon irradiation.

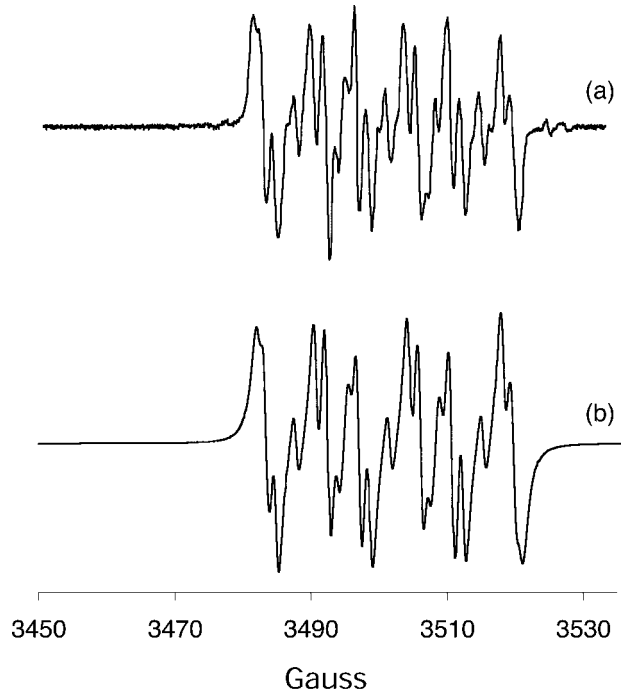

Figure 11. EPR spectra generated from irradiation of Emo and DMPO in aerated ethanol. (a) Irradiation with white light and (b) computer simulation; hfc's are given in Table 3. EPR conditions: microwave power, 10 mW; modulation amplitude, 0.22 G; receiver gain, 1×10^5; time constant, 0.32 s; scan range, 100 G; center of field, 3500 G; temperature, 25°C.

These observations are consistent with both schemes. According to criteria formulated by Eberson (54,61), the second mechanism seems to be the preferred one when photosensitizers are characterized by a redox potential in the triplet state >1.7–1.8 V (*vs* SCE). The Emo satisfied these criteria because its triplet redox potential is equal to about 2.0 V (*vs* SCE) (63).

Taking into account the redox potential values of amino acids such as tyrosine and tryptophan (0.7 and 0.81 V [*vs* SCE], [64]) and those of nucleic bases (0.92–1.62 V [*vs* SCE], [65]) we propose that Emo could oxidize proteins or nucleic acids once it penetrates into cells and is illuminated to generate its corresponding excited triplet state. The oxidation of proteins and nucleic acids would cause their degradation and deactivation eventually leading to the cell's death. Notably, the antiviral activity of the hypericin, *i.e.* the dimer of emodin was observed also under anaerobic conditions (66).

When the EPR spectrum of the mixture of [D-Lys^6(Emo)]GnRH DMPO and Fe(II) in aerated phosphate buffer (PB) containing 10% DMSO was recorded in the dark a six-line signal with the DMPO–CH_3 pattern appeared. This result indicates that [D-Lys^6(Emo)]GnRH could also generate a ROS-like Emo even in the dark. On the other hand, irradiation of [D-Lys^6(Emo)]GnRH and DMPO in aerated PB gave rise to the appearance of a weak EPR signal owing to the DMPO–OH adduct. The relatively low photochemical activity of [D-Lys^6(Emo)]GnRH compared with Emo could

be ascribed to the quenching effect of the aromatic side chain of [D-Lys^6]GnRH.

The stability of [D-Lys^6(Emo)]GnRH toward the highly reactive ROS radicals produced by its irradiation is a prerequisite for specific and efficient targeting. This aspect was evaluated by an HPLC study. According to EPR measurements OH radicals were formed when the mixture of [D-Lys^6(Emo)]GnRH in aerated PB containing 10% DMSO was irradiated for 20 min. The mixture was then analyzed by analytical HPLC. The HPLC results show that less than 3% of [D-Lys^6(Emo)]GnRH was degraded by the generation of ROS, similar to other cytotoxic derivatives of [D-Lys^6]GnRH (30).

CONCLUSIONS

The present study demonstrates the synthesis, electron-transfer behavior and photochemistry of Emo and its [D-Lys^6]GnRH derivative, [D-Lys^6(Emo)]GnRH, which was synthesized in a homogeneous solution. The conjugate preserves the biological activity of the parent peptide, *i.e.* binding to GnRH receptors and inducing LH release from pituitary cells.

The electrochemistry studies illustrated a redox potential of −0.59 V (*vs* SCE) for the first reduction step of emodin and Emo, which is less negative than the first redox potential of a well-known redox active compound, adriamycin (−0.665 V [*vs* SCE]).

The photochemical studies showed that upon irradiation Emo produces Emo semiquinone that is identical to semiquinones generated by chemical or electrochemical methods. Spin trapping experiments showed that upon irradiation, Emo and [D-Lys^6(Emo)]GnRH generate superoxide radicals, which in the presence of metal ions consequently cause the formation of highly reactive hydroxyl radicals. However, incorporation of Emo to [D-Lys^6]GnRH diminished its ability to generate the ROS. These findings, together with energy calculations, also suggest the formation of a strong oxidant, the triplet state of Emo (2.14 V [*vs* SCE]), which could directly lead to the oxidation of nucleic acids and proteins.

We conclude that Emo and its [D-Lys^6]GnRH conjugate may potentially be cytotoxic in a biological system in two different ways, simultaneously: first, dark cytotoxicity, which involves the generation of ROS by enzymatic reduction and second, phototoxicity through photogeneration of ROS or oxidation of nucleic acids and amino acids by corresponding excited triplet state species.

Acknowledgements—This work was supported by CaP CURE Israel.

REFERENCES

1. Powis, G. (1989) Free radical formation by antitumor quinones. *Free Radic. Biol. Med.* **6**, 63–101.
2. Palit, D. K., H. Pal, T. Mukherjee and J. J. P. Mittal (1990) Photodynamics of the S1 state of some hydroxy- and amino-substituted naphthoquinones and anthraquinones. *J. Chem. Soc. Faraday Trans.* **86**, 3861–3869.
3. Ashnagar, A., J. M. Bruce, P. L. Dutton and R. C. Prince (1984) One- and two-electron reduction of hydroxy-1,4-naphthoquinones and hydroxy- 9,10-anthraquinones. The role of internal hydrogen bonding and its bearing on the redox chemistry of the anthracycline antitumour quinones. *Biochim. Biophys. Acta* **801**, 351–359.
4. Weiner, L. M. (1994) Oxygen radicals generation and DNA scission by anticancer and synthetic quinones. *Methods Enzymol.* **233**, 92–105.
5. Pacifici, R. E. and K. J. A. Davies (1990) Protein degradation as an index of oxidative stress. *Methods Enzymol.* **186**, 485–502.
6. Burkitt, M. J., M. Fitchett and B. C. Gilbert (1989) Free-radical damage to nucleic acid components initiated by the Fenton reaction: an E.S.R. study. *Medical, biochemical and chemical aspects of free radicals.* (Edited by O. Hayaishi, E. Niki, M. Kondo and T. Yoshikawa), pp. 63–70. Elsevier Science Publishers, Amsterdam, Proceedings of the 4th Biennial General Meeting of the Society for Free Radical Research, Kyoto, Japan, 9–13 April 1988.
7. Stadtman, E. R. (1993) Oxidation of free amino acids and amino acid residues in proteins by radiolysis and by metal-catalyzed reactions. *Annu. Rev. Biochem.* **62**, 797–821.
8. Gollnick, K., S. Held, D. O. Martire and S. E. Braslavsky (1992) Hydroxyanthraquinones as sensitizers of singlet oxygen reactions: quantum yields of triplet formation and singlet oxygen generation in acetonitrile. *J. Photochem. Photobiol. A: Chem.* **69**, 155–165.
9. Dabestani, R., R. D. Hall, R. H. Sik and C. F. Chignell (1990) Spectroscopic studies of cutaneous photosensitizing agents–XV. Anthralin and its oxidation product 1,8-dihydroxyanthraquinone. *Photochem. Photobiol.* **52**, 961–971.
10. Thomas, C. and R. S. Pardini (1992) Oxygen dependence of hypericin-induced phototoxicity to EMT6 mouse mammary carcinoma cells. *Photochem. Photobiol.* **55**, 831–837.
11. Lavie, G., F. Valentine, B. Levin, Y. Mazur, G. Gallo, D. Lavie, D. Weiner and D. Meruelo (1989) Studies of the mechanisms of action of the antiretroviral agents hypericin and pseudohypericin. *Proc. Natl. Acad. Sci. USA* **86**, 5963–5967.
12. Hartman, P. E. and M. A. Goldstein (1989) Superoxide generation by photomediated redox cycling of anthraquinones. *Environ. Mol. Mutagen.* **14**, 42–47.
13. Mueller, S. O., W. K. Lutz and H. Stopper (1998) Factors affecting the genotoxic potency ranking of natural anthraquinones in mammalian cell culture systems. *Mutat. Res.* **414**, 125–129.
14. Morita, H., M. Umeda, T. Masuda and Y. Ueno (1988) Cytotoxic and mutagenic effects of emodin on cultured mouse carcinoma FM3A cells. *Mutat. Res.* **204**, 329–332.
15. Kawai, K., T. Kato, H. Mori, J. Kitamura and Y. Nozawa (1984) A comparative study on cytotoxicities and biochemical properties of anthraquinone mycotoxins emodin and skyrin from *Penicillium islandicum* Sopp. *Toxicol. Lett.* **20**, 155–160.
16. Westendorf, J., H. Marquardt, B. Poginsky, M. Dominiak, J. Schmidt and H. Marquardt (1990) Genotoxicity of naturally occurring hydroxyanthraquinones. *Mutat. Res.* **240**, 1–12.
17. Koyama, M., K. Takahashi, T. C. Chou, Z. Darzynkiewicz, J. Kapuscinski, T. R. Kelly and K. A. Watanabe (1989) Intercalating agents with covalent bond forming capability. A novel type of potential anticancer agents. 2. Derivatives of chrysophanol and emodin. *J. Med. Chem.* **32**, 1594–1599.
18. Zhang, L., Y. K. Lau, L. Xi, R. L. Hong, D. S. Kim, C. F. Chen, G. N. Hortobagyi, C. j. Chang and M. C. Hung (1998) Tyrosine kinase inhibitors, emodin and its derivative repress HER-2/neu-induced cellular transformation and metastasis-associated properties. *Oncogene* **16**, 2855–2863.
19. Kodama, M., Y. Kamioka, T. Nakayama, C. Nagata, N. Morooka and Y. Ueno (1987) Generation of free radical and hydrogen peroxide from 2-hydroxyemodin, a direct-acting mutagen, and DNA strand breaks by active oxygen. *Toxicol. Lett.* **37**, 149–156.
20. FitzGerald, D. and I. Pastan (1989) Targeted toxin therapy for the treatment of cancer. *J. Natl. Cancer Inst.* **81**, 1455–1463.
21. Eidne, K. A., C. A. Flanagan, N. S. Harris and R. P. Millar (1987) Gonadotropin-releasing hormone (GnRH)-binding sites in human breast cancer. *J. Clin. Endocrinol. Metab.* **64**, 425–432.
22. Halmos, G., J. M. Arencibia, A. V. Schally, R. Davis and D. G. Bostwick (2000) High incidence of receptors for luteinizing hormone-releasing hormone (LHRH) and LHRH receptor gene expression in human prostate cancers. *J. Urol.* **163**, 623–629.
23. Bajusz, S., T. Janaky, V. J. Csernus, L. Bokser, M. Fekete, G.

Srkalovic, T. W. Redding and A. V. Schally (1989) Highly potent analogues of luteinizing hormone-releasing hormone containing D-phenylalanine nitrogen mustard in position 6. *Proc. Natl. Acad. Sci. USA* **86**, 6318–6322.
24. Nagy, A., A. V. Schally, P. Armatis, K. Szepeshazi, G. Halmos, M. Kovacs, M. Zarandi, K. Groot, M. Miyazaki, A. Jungwirth and J. Horvath (1996) Cytotoxic analogs of luteinizing hormone-releasing hormone containing doxorubicin or 2-pyrrolinodoxorubicin, a derivative 500–1000 times more potent. *Proc. Natl. Acad. Sci. USA* **93**, 7269–7273.
25. Bajusz, S., T. Janaky, V. J. Csernus, L. Bokser, M. Fekete, G. Srkalovic, T. W. Redding and A. V. Schally (1989) Highly potent metallopeptide analogues of luteinizing hormone- releasing hormone. *Proc. Natl. Acad. Sci. USA* **86**, 6313–6317.
26. Janaky, T., A. Juhasz, S. Bajusz, V. Csernus, G. Srkalovic, L. Bokser, S. Milovanovic, T. W. Redding, Z. Rekasi, A. Nagy and A. V. Schally (1992) Analogues of luteinizing hormone-releasing hormone containing cytotoxic groups. *Proc. Natl. Acad. Sci. USA* **89**, 972–976.
27. Milovanovic, S. R., S. Radulovic and A. V. Schally (1993) Evaluation of binding of cytotoxic analogs of luteinizing hormone-releasing hormone to human breast cancer and mouse MXT mammary tumor. *Breast Cancer Res. Treat.* **24**, 147–158.
28. Buettner, G. R. and L. W. Oberley (1978) Considerations in the spin trapping of superoxide and hydroxyl radical in aqueous systems using 5,5-dimethyl-1-pyrroline-1-oxide. *Biochem. Biophys. Res. Commun.* **83**, 69–74.
29. Atherton, E. and R. C. Sheppard (1989) *Solid Phase Peptide Synthesis—A Practical Approach*. IRL Press, Oxford.
30. Rahimipour, S., L. Weiner, P. B. Shrestha-Dawadi, S. Bittner, Y. Koch and M. Fridkin (1998) Cytotoxic peptides: naphthoquinonyl derivatives of luteinizing hormone-releasing hormone. *Lett. Pept. Sci.* **5**, 421–427.
31. Meites, L., P. Zuman, W. J. Scott, B. H. Campbell, A. M. Kardos, T. L. Fenner, E. B. Rupp, L. Lampugani and R. Zuman (1976) *Handbook Series in Organic Elelectrochemistry*. CRC Press, Cleveland.
32. Gescheidt, G. (1994) A simple experimental setup for the simultaneous measurement of ESR and absorption spectra. *Rev. Sci. Instrum.* **65**, 2145–2146.
33. Phillips, A. H. and R. C. Langdon (1962) Hepatic triphosphopyridine nucleotide-cytochrome *c* reductase: isolation, characterization, and kinetic studies. *J. Biol. Chem.* **237**, 2652–2660.
34. Duling, D. R. (1994) Simulation of multiple isotropic spin-trap EPR-spectra. *J. Magn. Reson. B.* **104**, 105–110.
35. Becke, A. D. (1993) A new mixing of Hartree–Fock and local density-functional theories. *J. Chem. Phys.* **98**, 1372–1377.
36. Kohn, W., A. D. Becke and R. G. Parr (1996) Density functional theory of electronic structure. *J. Phys. Chem.* **100**, 12 974–12 980.
37. Stephens, P. J., F. J. Devlin, C. F. Chabalowski and M. J. Frisch (1994) Ab-initio calculation of vibrational absorption and circular-dichroism spectra using density-functional force-fields. *J. Phys. Chem.* **98**, 11 623–11 627.
38. Yahalom, D., S. Rahimipour, Y. Koch, N. Ben-Aroya and M. Fridkin (2000) Structure–activity studies of reduced-size gonadotropin-releasing hormone agonists derived from the sequence of an endothelin antagonist. *J. Med. Chem.* **43**, 2824–2830.
39. Rahimipour, S., N. Ben-Aroya, M. Fridkin and Y. Koch (2001) Design, synthesis and evaluation of a highly potent analog of gonadotropin-releasing hormone with prolong bioactivity. (In press)
40. Momany, F. A. (1976) Conformational energy analysis of the molecule, luteinizing hormone-releasing hormone. 1. Native decapeptide. *J. Am. Chem. Soc.* **98**, 2990–2996.
41. Nikiforovich, G. V. and G. R. Marshall (1993) Conformation–function relationships in LHRH analogs. *Int. J. Pept. Protein Res.* **42**, 171–180.
42. Batra, R., B. Giese, M. Spichty, G. Gescheidt and K. N. Houk (1996) Calculations of isotropic hyperfine coupling constants of organic radicals. An evaluation of semiempirical, Hartree–Fock, and density functional methods. *J. Phys. Chem.* **100**, 18 371–18 379.
43. Gauld, J. W., L. A. Eriksson and L. Radom (1997) Assessment of procedures for calculating radical hyperfine structures. *J. Phys. Chem. A* **101**, 1352–1359.
44. Svingen, B. A. and G. Powis (1981) Pulse radiolysis studies of antitumor quinones: radical lifetimes, reactivity with oxygen, and one-electron reduction potentials. *Arch. Biochem. Biophys.* **209**, 119–126.
45. Li, A. S. W. and C. F. Chignell (1987) Spectroscopic studies of cutaneous photosensitizing agents—X. A spin-trapping and direct electron spin resonance study of the photochemical pathways of daunomycin and adriamycin. *Photochem. Photobiol.* **45**, 565–570.
46. Buettner, G. R. (1987) Spin trapping: ESR parameters of spin adducts. *Free Radic. Biol. Med.* **3**, 259–303.
47. Finkelstein, E., G. M. Rosen and E. J. Rauckman (1980) Spin trapping. Kinetics of the reaction of superoxide and hydroxyl radicals with nitrones. *J. Am. Chem. Soc.* **102**, 4994–4999.
48. Finkelstein, E., G. M. Rosen and E. J. Rauckman (1982) Production of hydroxyl radical by decomposition of superoxide spin trapped adducts. *Mol. Pharmacol.* **21**, 262–265.
49. Chignell, C. F., A. G. Motten, R. H. Sik, C. E. Parker and K. Reszka (1994) A spin trapping study of the photochemistry of 5,5-dimethyl-1-pyrroline *N*-oxide (DMPO). *Photochem. Photobiol.* **59**, 5–11.
50. Dorfman, L. M. and G. E. Adams (1973) *Reactivity of the hydroxyl radical in aqueous solutions*. GPO, Washington, DC.
51. Finkelstein, E., G. M. Rosen, E. J. Rauckman and J. Paxton (1979) Spin trapping of superoxide. *Mol. Pharmacol.* **16**, 676–685.
52. Carmichael, A. J., M. M. Mossoba and P. Riesz (1983) Photogeneration of superoxide by adriamycin and daunomycin. An electron spin resonance and spin trapping study. *FEBS Lett.* **164**, 401–405.
53. Eberson, L., M. P. Hartshorn and O. Persson (1996) Inverted spin trapping. 5. 1,1,1,3,3,3-hexafluoropropan-2-ol as a solvent for the discrimination between proper and inverted spin trapping. *J. Chem. Soc. Perkin Trans 2* **2**, 141–149.
54. Eberson, L. (1998) Spin trapping and electron transfer. *Adv. Phys. Org. Chem.* **31**, 91–141.
55. Behar, D., G. Czapski, J. Rabani, L. M. Dorfman and H. A. Schwarz (1970) The acid dissiciation constant and decay kinetics of the perhydroxyl radical. *J. Phys. Chem.* **74**, 3209–3213.
56. Lauffer, B. L. (1992) *Iron and human disease*. CRC Press, Boca Raton.
57. Harbour, J. R., V. Chow and J. R. Bolton (1974) An electron spin resonance study of the spin adducts of OH and HO2 radicals with nitrones in the ultraviolet photolysis of aqueous hydrogen peroxide solutions. *Can. J. Chem.* **52**, 3549–3553.
58. Rosen, G. M. and E. J. Rauckman (1980) Spin trapping of the primary radical involved in the activation of the carcinogen *N*-hydroxy-2-acetylaminofluorene by cumene hydroperoxide-hematin. *Mol. Pharmacol.* **17**, 233–238.
59. Bilski, P., K. Reszka, M. Bilska and C. F. Chignell (1996) Oxidation of the spin trap 5,5-dimethyl-1-pyrroline *N*-oxide by singlet oxygen in aqueous solution. *J. Am. Chem. Soc.* **118**, 1330–1338.
60. Forrester, A. R. and S. P. Hepburn (1971) Spin traps. A cautionary note. *J. Chem. Soc. (C)* 701–703.
61. Eberson, L. (1999) Formation of hydroxyl spin adducts via nucleophilic addition-oxidation to 5,5-dimethyl-1-pyrroline *N*-oxide (DMPO). *Acta Chem. Scand.* **53**, 584–593.
62. Eberson, L., J. Lind and G. Merenyi (1994) Inverted spin trapping. Part IV. Application to the formation of imidyl spin adducts from *N*-haloimides. *J. Chem. Soc. Perkin Trans. 2* 1181–1188.
63. Julliard, M. and M. Chanon (1983) Photoelectron-transfer catalysis: its connections with thermal and electrochemical analogues. *Chem. Rev.* **83**, 425–506.
64. DeFelippis, M. R., C. P. Murthy, F. Broitman, D. Weinraub and M. Faraggi (1991) Electrochemical properties of tyrosine phenoxy and tryptophan indolyl radicals in peptides and amino acids analogues. *J. Phys. Chem.* **95**, 3416–3419.
65. Seidel, C. A. M., A. Schulz and M. H. M. Sauer (1996) Nucleobase-specific quenching of fluorescent dyes. 1. Nucleobase one-electron redox potentials and their correlation with static and dynamic quenching efficiencies. *J. Phys. Chem.* **100**, 5541–5553.
66. Park, J., D. S. English, Y. Wannemuehler, S. Carpenter and J. W. Petrich (1998) The role of oxygen in the antiviral activity of hypericin and hypocrellin. *Photochem. Photobiol.* **68**, 593–597.